Geometric Tracking Control of an Unmanned Aerial Vehicle Based On Variations in Center of Gravity

Lovro Marković, Antun Ivanović, Marko Car, Matko Orsag, Stjepan Bogdan

***Abstract*— This paper is focused on presenting the concept of geometric tracking control for an unmanned aerial vehicle (UAV) based on variations in center of gravity. It has the ability to exploit its dynamic center of mass as a means of stabilization and control. A mathematical model of such system will be given as grounds for developing the nonlinear geometric tracking controller on the special Euclidean group SE(3). It will be shown that the chosen control terms have desirable properties. Finally, two sets of Gazebo simulation results for a selected trajectory tracking problem using two unique UAV concepts will be presented.**

I. INTRODUCTION

Geometric control concept has previously been applied for classic quadrotor vehicles in [1], [2], [3] set up in plus configuration with their center of gravity located inside the origin of the UAV body frame. Since a specific type of UAV is considered in this paper, a different approach to modeling such a system will be taken. Unlike a standard UAV, it utilizes variations in its center of gravity in order to achieve attitude tracking. Essentially, this means that such variations, which would usually be considered a disturbance in the system, could be exploited as a means of controlling the UAV. One of the ways these variations will be achieved is by implementing the moving mass concept on the standard quadrotor UAV. This includes mounting moving blocks on the UAV axes, whose offset will act as the control input of the system along with rotor speed variation. This is a novel concept first developed in [4],[5] with attitude control considered in [6]. Up to this point, the concept of geometric control has not been applied to the moving-mass controlled UAV.

Another way such variations could be achieved is by mounting two manipulators to the UAV and having them carry a relatively heavy payload - compared to the total UAV mass. In this case position of the payload will directly determine any offset in center of gravity. UAVs endowed with manipulators have previously been studied in [7], [8]. Similar trajectory tracking problem has previously been presented in [9]. In this paper, however, two 3-DOF manipulators are used, each carrying a payload. They are considered as an extension of the UAV used only for attitude control and not the main subject for trajectory tracking.

Authors are with Faculty of Electrical and Computer Engineering, University of Zagreb, 10000 Zagreb, Croatia (Antun Ivanović, Marko Car, Tomislav Haus, Matko Orsag, Stjepan Bogdan, Lovro Marković) at fer.hr

Since the geometric controller is used in this paper, model dynamics need to be expressed on SE(3) configuration manifold. Similar quadrotor dynamics have already been considered in other research papers e.g. [1], [10], [3] in which center of gravity lies in the origin of the body-fixed frame. However, in this paper it is not the case. Due to the variations in center of gravity a different dynamic model will be taken in consideration.

Therefore, the goal of this paper is to present the appropriate dynamic model for UAVs with variable center of gravity on the SE(3) configuration manifold, chose control terms based on that model and evaluate controller performance on a predefined trajectory tracking problem using two different UAV models able to change their center of gravity.

UAV model used in Gazebo simulations will be μMORUS which is a scaled down version of a UAV used in the MORUS project [11].

The paper is organized as follows. First the general mathematical model will be presented on the SE(3) configuration manifold along with expressions for center of gravity and moments of inertia. Using that mathematical model, control terms will be chosen such that desirable error dynamics can be obtained. Sufficient stability conditions will be presented for the obtained error dynamics. Lastly, two sets of simulations will be conducted using the Gazebo simulator and ROS environment. A trajectory tracking problem will be given to both UAV models, results will be presented and compared.

II. Mathematical model

First of all, it is necessary to introduce a fixed inertial reference frame $\{\mathbf{e}_1, \mathbf{e}_2, \mathbf{e}_3\}$ and a body-fixed frame $\{\mathbf{b}_1, \mathbf{b}_2, \mathbf{b}_3\}$. As it was previously stated, one of the ways μMORUS UAV will exploit its shifting center of gravity (CoG) due to the moving masses in order to maneuver and stabilize itself. Therefore, a CoG vector from the origin of the body-fixed frame will be defined as follows:

$$\mathbf{r}_{CoG} = \frac{m_b \mathbf{r}_{0,b} + \sum_{i=1}^{n} m_i \mathbf{r}_i}{m_b + \sum_{i=1}^{4} m_i} = \frac{\sum_{i=1}^{4} m_i \mathbf{r}_i}{m_t}, \qquad (1)$$

The following terms are defined as:

- $\mathbf{r}_{CoG} \in \mathrm{R}^3$ - Center of gravity with respect to the body-fixed frame

- $\mathbf{r}_i \in \mathrm{R}^3$ - Position of the i-th mass w.r.t. the body-fixed frame
- $\mathbf{r}_b \in \mathrm{R}^3$ - Position of UAV body w.r.t. the body-fixed frame. Note that because the body frame origin coincides with the rigid body CoG (without considering the moving masses) this term yields $\mathbf{r}_b = 0_{3x1}$
- $m_b \in \mathbb{R}$ - Mass of the UAV body
- $m_i \in \mathbb{R}$ - Mass of the i-th moving mass attached to the UAV link
- $m_t \in \mathbb{R}$ - Mass of the whole UAV

When considering center of gravity in the case of UAV with the manipulator, due to the antisymmetric configuration of the links its effect on center of gravity gets mutually cancelled out. The remaining formula follows:

$$\mathbf{r}_{CoG} = \frac{m_p \mathbf{r}_l + m_p \mathbf{r}_r}{m_t} \tag{2}$$

where $\mathbf{r}_l \in \mathbb{R}^3$ and $\mathbf{r}_r \in \mathbb{R}^3$ are left and right gripper positions in the body-fixed frame.

Moment of inertia matrix expressed in the body-fixed frame is defined as follows:

$$J = J_b + \sum_{i=1}^{n} J_i \tag{3}$$

where J_b is body and J_i is moment of inertia of some mass element outside the origin of the body-fixed frame. Using the parallel axis theorem, one is able to calculate J_i while knowing moment of inertia around its CoG:

$$J_i = J_{i,CoG} + m_i(\mathbf{r}_i^T \cdot \mathbf{r}_i \mathrm{I}_{3\times 3} - \mathbf{r}_i \cdot \mathbf{r}_i^T) \tag{4}$$

Either four moving masses or the manipulator payload will be taken in consideration when calculating each moment of inertia.

The equations of motion expressed in the inertial frame while taking in consideration that the CoG is located outside the origin of the body-fixed frame are as follows[12]:

$$\dot{\mathbf{x}} = \mathbf{v} \tag{5}$$

$$m_t \dot{\mathbf{v}} + m_t g \mathbf{e}_3 - m_T \mathrm{R} \mathbf{r}_{CoG} \times \dot{\mathbf{\Omega}} - m_t \mathrm{R} \hat{\mathbf{\Omega}} \hat{\mathbf{r}}_{CoG} \mathbf{\Omega} = f \mathrm{R} \mathbf{e}_3 \tag{6}$$

$$\dot{\mathrm{R}} = \mathrm{R} \hat{\mathbf{\Omega}} \tag{7}$$

$$J \dot{\mathbf{\Omega}} + \mathbf{\Omega} \times J \mathbf{\Omega} + m_t \mathbf{r}_{CoG} \times \mathrm{R}^T \dot{\mathbf{v}} = \mathbf{M} \tag{8}$$

The *hat map* is an operator equivalent to the expression $\hat{x}y = \mathbf{x} \times y$. It maps elements of $\mathbb{R}^3$ to the so(3) Lie algebra.

The following terms are defined as:

- $J \in \mathbb{R}^{3\times 3}$ - Moment of inertia matrix w.r.t. the body-fixed frame
- $\mathrm{R} \in SO(3)$ - Rotation matrix from the body fixed frame to the inertial frame
- $\mathbf{\Omega} \in \mathbb{R}^3$ - Angular velocity in the body-fixed frame
- $\mathbf{x} \in \mathbb{R}^3$ - Location of the body-fixed frame in the inertial frame
- $\mathbf{v} \in \mathbb{R}^3$ - Velocity of the body-fixed frame in the inertial frame
- $f \in \mathbb{R}$ - Total thrust produced by the UAV
- $\mathbf{M} \in \mathbb{R}^3$ - Total moments acting in the body-fixed frame

Equations 5, 6, 7 and 8 describe the dynamical flow of a rotating and translating rigid body in terms of evolution of $(\mathrm{R}, \mathbf{x}, \mathbf{\Omega}, \dot{\mathbf{x}}) \in \mathrm{TSE}(3)$ on the tangent bundle of SE(3). It is important to note that the changes in moment of inertia and center of gravity have been omitted in favor of simplicity in equations 6 and 8. The complete model dynamics in the inertial frame are presented in the appendix.

Height and yaw of the UAV is controlled by variations in rotor velocity, whereas roll and pitch by variations in center of gravity. It is assumed that first and third propeller rotate clockwise, while second and fourth rotate counter-clockwise. The relation between moments, thrust and rotor velocity is the following:

$$f_i = b_f \omega_i^2 \tag{9}$$

$$\tau_i = (-1)^i b_m f_i \tag{10}$$

Where the following terms are defined as:

- $f_i \in \mathbb{R}$ - Thrust of the i-th motor
- $\tau_i \in \mathbb{R}$ - Moment i-th motor produces
- $b_f \in \mathbb{R}$ - Motor thrust constant
- $b_m \in \mathbb{R}$ - Motor moment constant
- $\omega_i \in \mathbb{R}$ - Rotation velocity of the i-th rotor

Total thrust can be expressed as:

$$f = \sum_{1}^{4} f_i \tag{11}$$

and total moment acting in the body-fixed frame as:

$$M = [m_1 g d_x \cdot b_{3,dx}, m_2 g d_y \cdot b_{3,dy}, b_m(-f_1 + f_2 - f_3 + f_4)] \tag{12}$$

Using f and M as control inputs of the system one is able to obtain the desired force of each rotor and the control offset d_x and d_y for either moving masses or the carried payload. While the control offsets are able to be directly applied as moving mass control inputs, in the manipulator case they will be converted to dq_1, dq_2, dq_3. Such conversion will be done using the inverse Jacobian of the manipulator end effector.5
Manipulator and moving mass actuator dynamics along with the change in desired rotor force will be regarded as instantaneous while presenting the controller synthesis and stability conditions. They will, however, be included within the Gazebo simulation environment.

III. Geometric control on SE(3)

In this section a nonlinear tracking controller will be developed. The main focus will be put on position tracking, therefore the trajectory will consist of a desired position $\mathbf{x}_d(t)$ and desired heading $\mathbf{b}_{1,d}$ of the body-fixed frame. Since the given position is known ahead of time, one is able to calculate both desired linear velocity $\mathbf{v}_d(t)$ and acceleration $\mathbf{a}_d(t)$ which will also inherently be included as inputs.
The controller will be developed on the nonlinear Lie group SE(3) whose subgroups are the rotation group SO(3) and translation group T(3). The main advantage of using the SO(3) rotation group is to avoid any singularities or ambiguities that may arise when representing rotations with Euler angles or quaternions.
Firstly, chosen position and orientation errors will be presented which will also lie on the SE(3) manifold and its tangent space. Using previously defined errors, nonlinear control terms can be chosen. Finally, the stability conditions of the tracking errors will be presented.

A. Tracking errors

Compatible attitude error function and transport map between tangent bundles of SO(3) are chosen as suggested in [13] and confirmed in research regarding geometric control with aerial vehicles [3], [10], [2], [1]. Attitude error function on SO(3) along with its compatible transport map are chosen as:

$$\Psi(\mathrm{R}, \mathrm{R}_d) = \frac{1}{2} tr[I - \mathrm{R}_d^T \mathrm{R}] \tag{13}$$

$$\mathcal{T}(\mathrm{R}, \mathrm{R}_d) = \mathrm{R}^T \mathrm{R}_d \tag{14}$$

Linear position and velocity tracking errors are defined as follows:

$$\mathbf{e}_x = \mathbf{x} - \mathbf{x}_d \tag{15}$$

$$\mathbf{e}_v = \mathbf{v} - \mathbf{v}_d \tag{16}$$

Defining attitude and angular velocity tracking errors is not as straight-forward. It is shown in [13] that the attitude tracking error should be chosen as a left-differential of the attitude error function $\Psi(\mathrm{R}, \mathrm{R}_d)$. It is chosen as follows:

$$\mathbf{e}_\mathrm{R} = \frac{1}{2}(\mathrm{R}_d^T \mathrm{R} - \mathrm{R}^T \mathrm{R}_d)^\vee \tag{17}$$

Due to the fact that angular velocities $\mathbf{\Omega} \in T_\mathrm{R} SO(3)$ and $\mathbf{\Omega}_d \in T_{\mathrm{R}_d} SO(3)$ lie in different tangential bundles, the proposed left transport map 14 needs to be applied when calculating the tracking error:

$$\mathbf{e}_\Omega = \mathbf{\Omega} - \mathrm{R}^T \mathrm{R}_d \mathbf{\Omega}_d \tag{18}$$

B. Control terms

Taking in consideration the proposed system dynamics 6 and 8, the force and moment control terms are chosen as follows:

$$\begin{aligned} \mathbf{A} = (&-\mathrm{k}_x \mathbf{e}_x - \mathrm{k}_v \mathbf{e}_v \\ &+ mg\mathbf{e}_3 + m\ddot{\mathbf{x}}_d \\ &- m\mathrm{R}\mathbf{r}_{CoG} \times \dot{\mathbf{\Omega}} - m\mathrm{R}\hat{\mathbf{\Omega}}\hat{\mathbf{r}}_{CoG}\mathbf{\Omega}) \\ f =& \mathbf{A} \cdot \mathrm{R}\mathbf{e}_3 \end{aligned} \tag{19}$$

$$\begin{aligned} \mathbf{M} = &-\mathrm{k}_\mathrm{R}\mathbf{e}_\mathrm{R} - \mathrm{k}_\Omega \mathbf{e}_\Omega \\ &+ \mathbf{\Omega} \times J\mathbf{\Omega} - J(\hat{\mathbf{\Omega}}\mathrm{R}^T\mathrm{R}_d\mathbf{\Omega}_d - \mathrm{R}^T\mathrm{R}_d\dot{\mathbf{\Omega}}_d) \\ &+ m\mathbf{r}_{CoG} \times \mathrm{R}^T\ddot{\mathbf{x}} \end{aligned} \tag{20}$$

When error dynamics will be presented, it can be seen that the control terms are chosen in order to negate the undesirable system dynamics.

Desired rotation matrix is constructed in the traditional way when considering geometric control of aerial vehicles [1], [2], [10]. The proposed desired rotation matrix is constructed as $\mathrm{R}_d = [\mathbf{b}_{1,c}, \mathbf{b}_{3,d} \times \mathbf{b}_{1,c}, \mathbf{b}_{3,d}]$ where component vectors of R_d are calculated in the following way:

$$\mathbf{b}_{3,d} = \frac{\mathbf{A}}{||\mathbf{A}||} \tag{21}$$

$$\mathbf{b}_{1,c} = -\frac{(\mathbf{b}_{3,d} \times (\mathbf{b}_{3,d} \times \mathbf{b}_{1,d}))}{||\mathbf{b}_{3,d} \times \mathbf{b}_{1,d}||} \tag{22}$$

It is also assumed that:

$$||\mathbf{A}|| \neq 0 \tag{23}$$

The chosen constraint for the trajectory tracking problem differs slightly from the one proposed in [1] due to the fact that different model dynamics are considered in this paper. New trajectory constraints are presented as follows:

$$||mge_3 + m\ddot{\mathbf{x}}_d - m\mathrm{R}\mathbf{r}_{CoG} \times \dot{\mathbf{\Omega}} - m\mathrm{R}\hat{\mathbf{\Omega}}\hat{\mathbf{r}}_{CoG}\mathbf{\Omega}|| < B \tag{24}$$

where B is some positive constant.

Desired angular velocity and acceleration also need to be considered in this trajectory tracking problem. One is able to calculate the desired angular velocity and acceleration using R_d and its derivatives in the following way:

$$\hat{\mathbf{\Omega}}_d = \mathrm{R}_d^T \dot{\mathrm{R}}_d \tag{25}$$

$$\dot{\hat{\mathbf{\Omega}}}_d = -\hat{\mathbf{\Omega}}_d\hat{\mathbf{\Omega}}_d + \mathrm{R}_d^T\ddot{\mathrm{R}}_d \tag{26}$$

Derivatives of R_d are easily calculated using the backwards differentiation method. It has to be noted that due to stability issues, computation rate of desired angular velocity and acceleration has to be lesser than the overall simulation rate. For further implementation details, please refer to [14].

C. Error dynamics and stability discussion

In this section linear and angular error dynamics will be presented. First of all, derivatives over time need to be calculated for linear 16 and angular 18 tracking errors:

$$\mathbf{e}_v = \dot{\mathbf{x}} - \dot{\mathbf{x}}_d \tag{27}$$

$$\mathbf{e}_\Omega = \dot{\mathbf{\Omega}} + \hat{\mathbf{\Omega}}\mathrm{R}^T\mathrm{R}_d\mathbf{\Omega}_d - \mathrm{R}^T\mathrm{R}_d\dot{\mathbf{\Omega}}_d \tag{28}$$

After including 6 and 8 in 27 and 28 respectively, the following equations are obtained:

$$\begin{aligned} m\mathbf{e}_v =& -mg\mathbf{e}_3 - m\ddot{\mathbf{x}}_d \\ &+ m\mathrm{R}\mathbf{r}_{CoG}\times\dot{\mathbf{\Omega}} + m\mathrm{R}\hat{\mathbf{\Omega}}\hat{\mathbf{r}}_{CoG}\mathbf{\Omega} \\ &+ \mathbf{A} + \mathbf{X} \end{aligned} \tag{29}$$

$$\begin{aligned} J\mathbf{e}_\Omega =& \mathbf{M} - \mathbf{\Omega}\times J\mathbf{\Omega} \\ &+ J(\hat{\mathbf{\Omega}}\mathrm{R}^T\mathrm{R}_d\mathbf{\Omega}_d - \mathrm{R}^T\mathrm{R}_d\dot{\mathbf{\Omega}}_d) \\ &+ m\mathbf{r}_{CoG}\times\mathrm{R}^T\ddot{\mathbf{x}} \end{aligned} \tag{30}$$

Note that in 29 $\mathbf{A}\in\mathrm{R}^3$ is regarded as a control force for the translational dynamics, mentioned in 19, while $\mathbf{X}\in\mathrm{R}^3$ is a bounded term that arises when deriving this equation which equals:

$$\mathbf{X} = \frac{f}{(\mathrm{R}_d\mathbf{e}_3)^T\mathrm{R}\mathbf{e}_3}(\mathrm{R}_d\mathbf{e}_3 - ((\mathrm{R}_d\mathbf{e}_3)^T\mathrm{R}\mathbf{e}_3)\mathrm{R}\mathbf{e}_3) \tag{31}$$

After substituting control force from 19 and 20 in 29 and 30 respectively the final form of error dynamics is obtained:

$$m\mathbf{e}_v = -k_x\mathbf{e}_x - k_v\mathbf{e}_v + \mathbf{X} \tag{32}$$

$$J\mathbf{e}_\Omega = -k_\mathrm{R}\mathbf{e}_\mathrm{R} - \mathrm{k}_\Omega\mathbf{e}_\Omega \tag{33}$$

Having started with a different mathematical model of the UAV than the previous research done on this subject, applying the newly formed control terms 19 and 20 and taking in consideration initial assumptions 23 and 24 one is able to derive identical translational and rotational error dynamics as found in [3], [1].
Therefore, to avoid redundancy, the full stability proof will not be presented in this paper. However, the final conclusions for exponential asymptotic stability of the attitude error function and attraction to the zero-equilibrium state of tracking errors will be outlined.

If the initial UAV configuration satisfies the following conditions:

$$\Psi(\mathrm{R}(0),\mathrm{R}_d(0)) < 2 \tag{34}$$

$$||\mathbf{e}_\Omega(0)||^2 < \frac{2}{\lambda_{min}(J)}k_\mathrm{R}(2-\Psi(\mathrm{R}(0),\mathrm{R}_d(0)) \tag{35}$$

it can be shown that tracking errors of the whole system will reach zero-equilibrium state and the attitude function will be exponentially bounded as:

$$\Psi(\mathrm{R}(t),\mathrm{R}_d(t)) \le \min\{2, \alpha e^{-\beta t}\} \tag{36}$$

for some positive constants α and β.

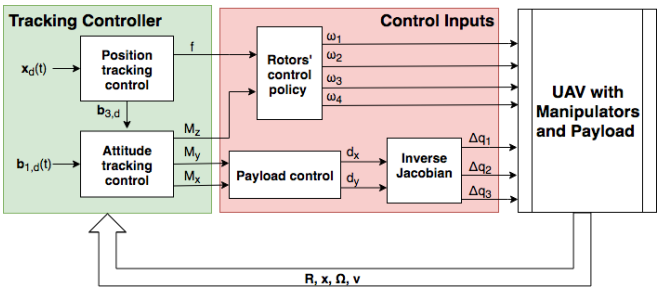

Fig. 1: Control scheme for the case of UAV carrying the payload. It is important to note that for the case of UAV with moving masses, *Inverse Jacobian* block will be omitted and control inputs d_x and d_y will be directly sent to the moving mass actuators.

IV. Simulation

In this section simulation results will be presented and analysed. Simulations are conducted in the Gazebo simulator within the ROS environment. UAV used in experiments is the μMorus which can be found in the *mmuav_gazebo* repository [14], along with its parameters. Two experiments will be conducted with different methods of CoG variation:

- UAV control based on moving masses
- UAV control based on payload carried by manipulator arms

Control parameters for the first case are chosen as follows:

$$\mathrm{k}_x = \begin{bmatrix} 10 & 0 & 0 \\ 0 & 10 & 0 \\ 0 & 0 & 50 \end{bmatrix}, \mathrm{k}_v = \begin{bmatrix} 3.75 & 0 & 0 \\ 0 & 3.75 & 0 \\ 0 & 0 & 20 \end{bmatrix}$$

$$\mathrm{k}_R = \begin{bmatrix} 1.5 & 0 & 0 \\ 0 & 1.5 & 0 \\ 0 & 0 & 10 \end{bmatrix}, \mathrm{k}_\Omega = \begin{bmatrix} 0.65 & 0 & 0 \\ 0 & 0.65 & 0 \\ 0 & 0 & 1.54 \end{bmatrix}$$

Rotational control parameters, in the second case, stay the same, while translational parameters are the following:

$$\mathrm{k}_x = \begin{bmatrix} 6 & 0 & 0 \\ 0 & 6 & 0 \\ 0 & 0 & 50 \end{bmatrix}, \mathrm{k}_v = \begin{bmatrix} 2.5 & 0 & 0 \\ 0 & 2.5 & 0 \\ 0 & 0 & 20 \end{bmatrix}$$

For both cases, initial parameters are obtained by considering the error dynamics 32 and 33 in the equilibrium state. However, they are further tuned for better performance.
It is important to note that the actuator dynamics of the moving masses is taken in consideration within the Gazebo simulation environment. Furthermore there is a slight transient delay when increasing or decreasing rotor velocity which results in a non-instantaneous control force change. These phenomena were not taken in consideration while modeling the system and choosing

control terms.

The chosen trajectory tracking problem is formulated as a rotating spiral:

$$\mathbf{x}_d(t) = [0.4\mathrm{t};\ 0.5\sin(\pi\mathrm{t});\ 0.6\cos(\pi\mathrm{t}) + 2]$$
$$\mathbf{b}_{1,d}(t) = [\cos\left(\frac{\pi}{5}\mathrm{t}\right);\ \sin\left(\frac{\pi}{5}\mathrm{t}\right);\ 0]$$

In the first case the total trajectory time is 20s while in the second case it will last 30s. Initial position and orientation is chosen at the start of the trajectory.

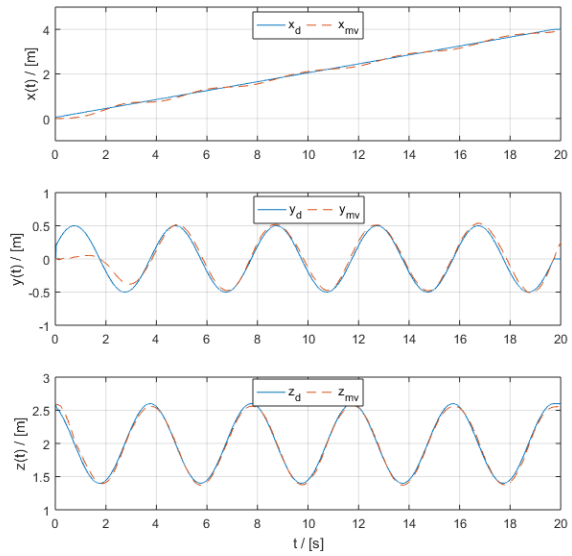

Fig. 2: Comparison of the desired $\mathbf{x}_d$ and measured position values $\mathbf{x}_{mv}$. (Using the moving mass control concept.)

V. Conclusion

Geometric control was presented and implemented for two separate UAV models with variable centers of gravity. Although the controller has been constructed without actuator dynamics in mind, during the simulations its effect can be seen. Trajectory problem given to the manipulator controlled UAV had to be somewhat slower in order to be successfully completed. Even still, worse performance can be observed in manipulator controlled UAV 5 compared to the moving mass UAV 2. The main reason for such behavior is the considerably slower actuator dynamics for mounted manipulators. As a result the carried payload will produce much slower change in center of gravity than moving masses.

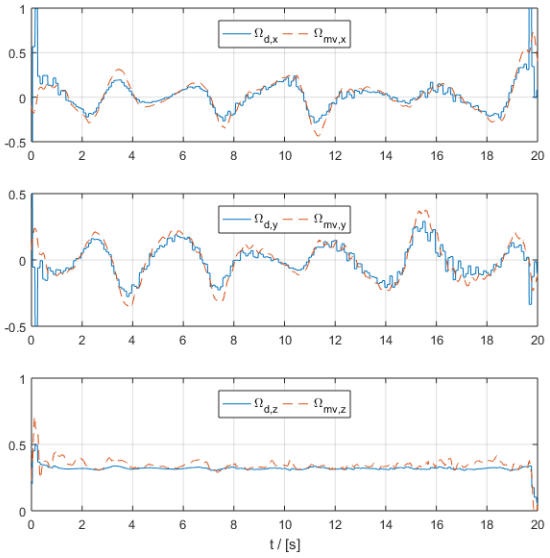

Fig. 3: Comparison of desired $\mathbf{\Omega}_d$ and measured $\mathbf{\Omega}_{mv}$ angular velocity values. (Using the moving mass control concept.)

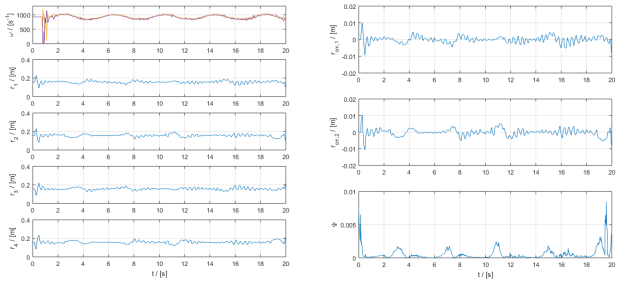

a) b)

Fig. 4: Control inputs are shown in figure a) in the following order: rotor velocities ω_i and mass offsets r_i. Figure b) shows first two components of CoG vector $\mathbf{r}_{CoG}$ (third component is always zero since masses only move in x-y plane of the body-fixed frame) and attitude error function Ψ. (Using the moving mass control concept.)

APPENDIX

A. UAS dynamics

In this section rotating body dynamics with variations in center of gravity will be derived. General form of Euler-Lagrange dynamics for a rotating rigid body in SE(3) configuration manifold in the body-fixed frame as

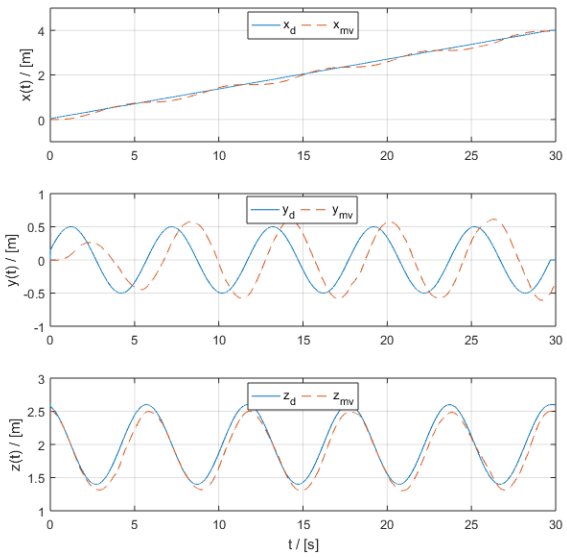

Fig. 5: Comparison of the desired $\mathbf{x}_d$ and measured position values $\mathbf{x}_{mv}$. (Using the manipulator control control.)

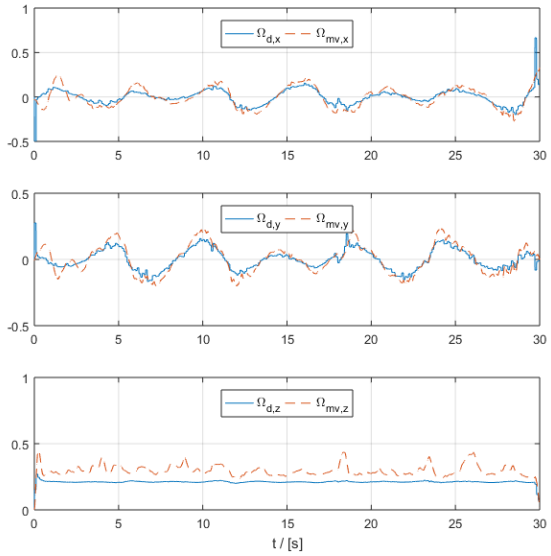

Fig. 6: Comparison of desired $\mathbf{\Omega}_d$ and measured $\mathbf{\Omega}_{mv}$ angular velocity values. (Using the manipulator control concept)

presented in [12]:

$$\frac{d}{dt}\left(\frac{\partial \mathcal{L}}{\partial \mathbf{\Omega}}\right) + \mathbf{\Omega} \times \frac{\partial \mathcal{L}}{\partial \mathbf{\Omega}} + \mathbf{v} \times \frac{\partial \mathcal{L}}{\partial \mathbf{v}} + \sum_{i=1}^{3} \mathbf{r}_i \times \frac{\partial \mathcal{L}}{\partial \mathbf{r}_i} = 0 \tag{37}$$

$$\frac{d}{dt}\left(\frac{\partial \mathcal{L}}{\partial \mathbf{v}}\right) + \mathbf{\Omega} \times \frac{\partial \mathcal{L}}{\partial \mathbf{v}} - \mathrm{R}^T \frac{\partial \mathcal{L}}{\partial x} = 0 \tag{38}$$

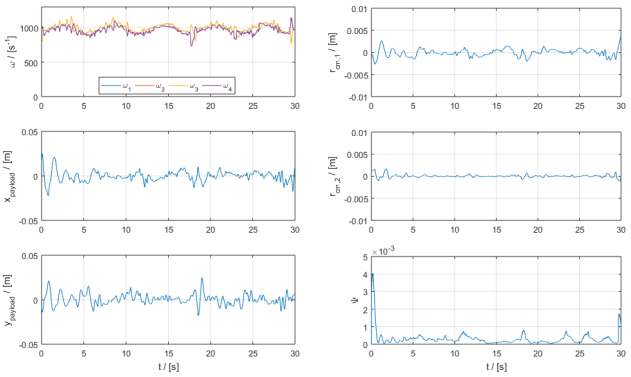

a) b)

Fig. 7: Control inputs: rotor velocities ω_i and payload position; are shown in in figure a). Figure b) shows first two components of CoG vector $\mathbf{r}_{CoG}$ and attitude error function Ψ.

For the the proposed UAS with variations in center of mass the Lagrangian is:

$$\mathcal{L}(\mathrm{R}, x, \mathbf{\Omega}, \mathbf{v}) = \frac{1}{2}\mathbf{\Omega}^T J \mathbf{\Omega} + m\mathbf{\Omega}^T \hat{\mathbf{r}}_{cm}\mathbf{v} + \frac{1}{2}m\mathbf{v}^T\mathbf{v} - U(\mathrm{R}, \mathbf{x}) \tag{39}$$

where $U(\mathrm{R}, \mathbf{x})$ is the potential energy of the system. It is important to note that J and $\mathbf{r}_{cm}$ are variable over time. Lagrangian derivatives needed for the general form equations 37 and 38 are:

$$\frac{\partial \mathcal{L}}{\partial \mathbf{\Omega}} = J\mathbf{\Omega} + m\hat{\mathbf{r}}_{cm})\mathbf{v} \tag{40}$$

$$\frac{d}{dt}\left(\frac{\partial \mathcal{L}}{\partial \mathbf{\Omega}}\right) = \dot{J}\mathbf{\Omega} + J\dot{\mathbf{\Omega}} + m\dot{\mathbf{r}}_{cm} \times \mathbf{v} + m\mathbf{r}_{cm} \times \dot{\mathbf{v}} \tag{41}$$

$$\frac{\partial \mathcal{L}}{\partial \mathbf{v}} = m\mathbf{v} - m\mathbf{r}_{cm} \times \mathbf{\Omega} \tag{42}$$

$$\frac{d}{dt}\left(\frac{\partial \mathcal{L}}{\partial \mathbf{v}}\right) = m\dot{\mathbf{v}} - m\dot{\mathbf{r}}_{cm} \times \mathbf{\Omega} - m\mathbf{r}_{cm} \times \dot{\mathbf{\Omega}} \tag{43}$$

It is of interest to transfer rotation and translation dynamics in the inertial frame. This can be done using the following relations:

$$\mathbf{v} = \mathrm{R}^T \dot{x} \tag{44}$$

$$\dot{\mathbf{v}} = \mathrm{R}^T \ddot{\mathbf{x}} - \mathbf{\Omega} \times (\mathrm{R}^T \dot{\mathbf{x}}) \tag{45}$$

$$\mathbf{r}_{cm} = \mathrm{R}^T(\mathbf{x}_{cm} - \mathbf{x}) \tag{46}$$

$$\dot{\mathbf{r}}_{cm} = \mathrm{R}^T(\dot{\mathbf{x}}_{cm} - \dot{\mathbf{x}}) + \mathrm{R}^T\hat{\mathbf{\Omega}}\mathbf{x}_{cm} - \hat{\mathbf{\Omega}}\mathrm{R}^T(\mathbf{x}_{cm} - \mathbf{x}) \tag{47}$$

After plugging in 40, 41, 42, 43 in 37, 38 and using 44, 45 as transformations of velocity and acceleration to

inertial frame the following equations are obtained:

$$\begin{aligned} &J\dot{\boldsymbol{\Omega}} + m\mathbf{r}_{cm} \times \mathrm{R}^T\ddot{\mathbf{x}} \\ &+ \dot{J}\boldsymbol{\Omega} + m\dot{\mathbf{r}}_{cm} \times \mathrm{R}^T\dot{\mathbf{x}} \\ &+ \boldsymbol{\Omega} \times J\boldsymbol{\Omega} + \sum_{i=1}^{3} \mathbf{r}_i \times \frac{\partial \mathcal{L}}{\partial \mathbf{r}_i} = 0 \end{aligned} \tag{48}$$

$$\begin{aligned} &m\ddot{\mathbf{x}} - m\mathrm{R}\hat{\mathbf{r}}_{cm}\dot{\boldsymbol{\Omega}} - m\mathrm{R}\hat{\mathbf{r}}_{cm}\boldsymbol{\Omega} \\ &- m\mathrm{R}\hat{\boldsymbol{\Omega}}\hat{\mathbf{r}}_{cm}\boldsymbol{\Omega} + \frac{\partial U}{\partial \mathbf{x}} = 0 \end{aligned} \tag{49}$$

After plugging in the center of mass transform 46, 47 the final form of dynamics is obtained:

$$\begin{aligned} &J\dot{\boldsymbol{\Omega}} + m\mathrm{R}^T(\mathbf{x}_{cm} - \mathbf{x}) \times \mathrm{R}^T\ddot{\mathbf{x}} + \dot{J}\boldsymbol{\Omega} \\ &+ m\widehat{\mathrm{R}^T\dot{\mathbf{x}}_{cm}}\mathrm{R}^T\dot{\mathbf{x}} - \mathrm{R}^T\dot{\mathbf{x}} \times (\mathrm{R}^T\hat{\boldsymbol{\Omega}}\mathbf{x}_{cm}) \\ &- m\hat{\boldsymbol{\Omega}}\mathrm{R}^T(\mathbf{x}_{cm} - \mathbf{x}) \times \mathrm{R}^T\dot{\mathbf{x}} \\ &+ \boldsymbol{\Omega} \times J\boldsymbol{\Omega} + \sum_{i=1}^{3} \mathbf{r}_i \times \frac{\partial \mathcal{L}}{\partial \mathbf{r}_i} = 0 \end{aligned} \tag{50}$$

$$\begin{aligned} &m\ddot{\mathbf{x}} - m\mathrm{R}\widehat{\mathrm{R}^T(\mathbf{x}_{cm} - \mathbf{x})}\dot{\boldsymbol{\Omega}} \\ &- m\mathrm{R}\widehat{\mathrm{R}^T(\dot{\mathbf{x}}_{cm} - \dot{\mathbf{x}})}\boldsymbol{\Omega} \\ &- m\mathrm{R}\widehat{\mathrm{R}^T\hat{\boldsymbol{\Omega}}\mathbf{x}_{cm}}\boldsymbol{\Omega} \\ &+ \frac{\partial U}{\partial \mathbf{x}} = 0 \end{aligned} \tag{51}$$

ACKNOWLEDGMENT

This research was supported in part by NATO's Emerging Security Challenges Division in the framework of the Science for Peace and Security Programme as Multi Year Project under G. A. number 984807, named Unmanned system for maritime security and environmental monitoring - MORUS.

References

[1] T. Lee, M. Leok, and N. H. McClamroch, "Geometric tracking control of a quadrotor uav on se(3)," in *49th IEEE Conference on Decision and Control (CDC)*, pp. 5420–5425, Dec 2010.

[2] T. Lee, M. Leok, and N. Harris McClamroch, "Nonlinear Robust Tracking Control of a Quadrotor UAV on SE(3)," *ArXiv e-prints*, Sept. 2011.

[3] T. Lee, M. Leok, and N. Harris McClamroch, "Control of Complex Maneuvers for a Quadrotor UAV using Geometric Methods on SE(3)," *ArXiv e-prints*, Mar. 2010.

[4] T. Haus, M. Orsag, and S. Bogdan, "Design considerations for a large quadrotor with moving mass control," in *2016 International Conference on Unmanned Aircraft Systems (ICUAS)*, pp. 1327–1334, June 2016.

[5] T. Haus, M. Orsag, and S. Bogdan, "Mathematical modelling and control of an unmanned aerial vehicle with moving mass control concept," *Journal of Intelligent & Robotic Systems*, vol. 88, pp. 219–246, Dec 2017.

[6] T. Haus, N. Prkut, K. Borovina, B. Marić, M. Orsag, and S. Bogdan, "A novel concept of attitude control for large multirotor-uavs based on moving mass control," in *2016 24th Mediterranean Conference on Control and Automation (MED)*, pp. 832–839, June 2016.

[7] M. Orsag, C. Korpela, S. Bogdan, and P. Oh, "Dexterous aerial robots—mobile manipulation using unmanned aerial systems," *IEEE Transactions on Robotics*, vol. 33, pp. 1453–1466, Dec 2017.

[8] C. Korpela, M. Orsag, M. Pekala, and P. Oh, "Dynamic stability of a mobile manipulating unmanned aerial vehicle," in *2013 IEEE International Conference on Robotics and Automation*, pp. 4922–4927, May 2013.

[9] H. Yang and D. Lee, "Dynamics and control of quadrotor with robotic manipulator," in *2014 IEEE International Conference on Robotics and Automation (ICRA)*, pp. 5544–5549, May 2014.

[10] T. Fernando, J. Chandiramani, T. Lee, and H. Gutierrez, "Robust adaptive geometric tracking controls on so(3) with an application to the attitude dynamics of a quadrotor uav," in *2011 50th IEEE Conference on Decision and Control and European Control Conference*, pp. 7380–7385, Dec 2011.

[11] "Morus project." `http://www.fer.unizg.hr/morus`. Accessed: 2017-09-08.

[12] T. Lee, M. Leok, and N. H. McClamroch, *Global formulations of Lagrangian and Hamiltonian dynamics on manifolds : a geometric approach to modeling and analysis*. Interaction of mechanics and mathematics series, Springer, 2018.

[13] A. D. L. Francesco Bullo, *Geometric control of mechanical systems: modeling, analysis, and design for simple mechanical control systems*. Texts in applied mathematics 49, Springer, 1 ed., 2005.

[14] "mmuav gazebo." `https://github.com/larics/mmuav_gazebo/tree/geometry_control`, 2018.

[15] A. D. L. Francesco Bullo, *Geometric control of mechanical systems: modeling, analysis, and design for simple mechanical control systems*. Texts in applied mathematics 49, Springer, 1 ed., 2005.

[16] F. P. Schuller, *Lectures on the Geometric Anatomy of Theoretical Physics*. Friedrich-Alexander-Universität Erlangen-Nürnberg, Institut für Theoretische Physik III, 2017.